AMERICAN SOCIETY FOR MICROBIOLOGY | Journal of Virology

Ecotropic Murine Leukemia Virus Infection of Glial Progenitors Interferes with Oligodendrocyte Differentiation: Implications for Neurovirulence

Ying Li,[a] Jaclyn M. Dunphy,[a,b] Carlos E. Pedraza,[c] Connor R. Lynch,[a] Sandra M. Cardona,[a,b] Wendy B. Macklin,[d] William P. Lynch[a,b]

Department of Integrative Medical Sciences, Northeast Ohio Medical University, Rootstown, Ohio, USA[a]; Programs in Neurosciences, and Cell and Molecular Biology, School of Biomedical Sciences, Kent State University, Kent, Ohio, USA[b]; EMD Serono Research and Development Institute, Inc., Billerica, Massachusetts, USA[c]; Department of Cell and Developmental Biology, University of Colorado School of Medicine, Aurora, Colorado, USA[d]

ABSTRACT

Certain murine leukemia viruses (MLVs) are capable of inducing fatal progressive spongiform motor neuron disease in mice that is largely mediated by viral Env glycoprotein expression within central nervous system (CNS) glia. While the etiologic mechanisms and the glial subtypes involved remain unresolved, infection of NG2 glia was recently observed to correlate spatially and temporally with altered neuronal physiology and spongiogenesis. Since one role of NG2 cells is to serve as oligodendrocyte (OL) progenitor cells (OPCs), we examined here whether their infection by neurovirulent (FrCasE) or nonneurovirulent (Fr57E) ecotropic MLVs influenced their viability and/or differentiation. Here, we demonstrate that OPCs, but not OLs, are major CNS targets of both FrCasE and Fr57E. We also show that MLV infection of neural progenitor cells (NPCs) in culture did not affect survival, proliferation, or OPC progenitor marker expression but suppressed certain glial differentiation markers. Assessment of glial differentiation *in vivo* using transplanted transgenic NPCs showed that, while MLVs did not affect cellular engraftment or survival, they did inhibit OL differentiation, irrespective of MLV neurovirulence. In addition, in chimeric brains, where FrCasE-infected NPC transplants caused neurodegeneration, the transplanted NPCs proliferated. These results suggest that MLV infection is not directly cytotoxic to OPCs but rather acts to interfere with OL differentiation. Since both FrCasE and Fr57E viruses restrict OL differentiation but only FrCasE induces overt neurodegeneration, restriction of OL maturation alone cannot account for neuropathogenesis. Instead neurodegeneration may involve a two-hit scenario where interference with OPC differentiation combined with glial Env-induced neuronal hyperexcitability precipitates disease.

IMPORTANCE

A variety of human and animal retroviruses are capable of causing central nervous system (CNS) neurodegeneration manifested as motor and cognitive deficits. These retroviruses infect a variety of CNS cell types; however, the specific role each cell type plays in neuropathogenesis remains to be established. The NG2 glia, whose CNS functions are only now emerging, are a newly appreciated viral target in murine leukemia virus (MLV)-induced neurodegeneration. Since one role of NG2 glia is that of oligodendrocyte progenitor cells (OPCs), we investigated here whether their infection by the neurovirulent MLV FrCasE contributed to neurodegeneration by affecting OPC viability and/or development. Our results show that both neurovirulent and nonneurovirulent MLVs interfere with oligodendrocyte differentiation. Thus, NG2 glial infection could contribute to neurodegeneration by preventing myelin formation and/or repair and by suspending OPCs in a state of persistent susceptibility to excitotoxic insult mediated by neurovirulent virus effects on other glial subtypes.

A variety of murine leukemia viruses (MLVs) are capable of inducing noninflammatory neurodegeneration upon infection of the central nervous system (CNS) (1–3). Depending on the virus, infected mice exhibit disease with variable incubation periods and clinical severity, initially manifesting as tremulous paralysis that progresses to decerebrate rigidity with associated wasting, which invariably leads to death (4, 5). Neurodegeneration is usually characterized by neuronal and glial vacuolation accompanied by gliosis that resembles the neuropathology seen in the prion-induced transmissible spongiform encephalopathies (6, 7). The prototypic neurovirulent MLV (NV), CasBrE, was first isolated from the brains of trapped wild mice and was shown by Gardner and colleagues (1) to be transmissible to several laboratory strains of mice. The primary neurovirulence determinants were mapped to the *env* gene (5, 8), and it has been subsequently demonstrated that Env is necessary and sufficient for neurodegeneration (9–11). Importantly, only mice infected with NVs during the neonatal period develop spongiform neurodegeneration, while mice infected at later times do not develop neuropathology due to a failure of virus to enter and spread within the CNS (12, 13). MLV-induced vacuolar changes are primarily observed in motor system neurons (14–16), with lesions predominantly involving swollen

Received 15 December 2015 **Accepted** 5 January 2016

Accepted manuscript posted online 13 January 2016

Citation Li Y, Dunphy JM, Pedraza CE, Lynch CR, Cardona SM, Macklin WB, Lynch WP. 2016. Ecotropic murine leukemia virus infection of glial progenitors interferes with oligodendrocyte differentiation: implications for neurovirulence. J Virol 90:3385–3399. doi:10.1128/JVI.03156-15.

Editor: B. Caughey

Address correspondence to William P. Lynch, wonk@neomed.edu.

Y.L. and J.M.D. contributed equally to this work.

postsynaptic terminals (14, 17). As pathology progresses, glial vacuolation and degeneration are also observed (15, 16, 18, 19).

MLVs infect many different CNS cell types, including postnatally proliferating neurons, neuroglia, microglia, and vascular endothelial cells; however, the postmitotic neurons that undergo degenerative changes appear refractory to infection. NVs and nonneurovirulent MLVs (NNs) with the same host range show no CNS cellular-tropism differences (14, 20–22), indicating that neurodegeneration results from the expression of unique neurovirulent Env conformers within one or more neuronal support cells. The questions of which neural cells are important and how they alter neuronal function remain largely unresolved.

Neurovirulent MLV infection of oligodendrocytes (OLs) has been reported by multiple groups based on morphological (14–16, 23–25) and immunological (19, 23) assessments; however, the frequency of OL infection was low, and its association with spongiosis was limited (10). These findings were consistent with the lack of overt white matter changes observed at the light microscopic level; however, myelin splitting has been noted at the ultrastructural level, raising the question of whether OL infection is involved in precipitating disease (5, 23). Clase et al. reported that glial cellular vacuolation characterized by watery cytoplasms but morphologically normal nuclei (referred to as cytoplasmic effacement [16]) primarily occurred within cells expressing Olig2 (19), a transcription factor specifying OL fate in the postnatal mouse (26). Because some morphologically normal Olig2$^+$ cells were observed to express viral protein, it was suggested that virus infection may lead directly to the cytoplasmic effacement of Olig2$^+$ cells (19). Because Olig2 expression is found at multiple stages of OL differentiation, it could not be determined whether cytoplasmic effacement represented damage to mature or immature glia or whether virus infection directly caused OL cytotoxicity.

OL progenitor cells (OPCs) proliferate and differentiate toward OLs during the postnatal period, peaking in the second postnatal week. One OPC marker, NG2, is a chondroitin sulfate proteoglycan first described by Stallcup that has been used to define a novel subpopulation of glia that exist in the adult and developing brain (27, 28; reviewed in reference 29). The adult NG2 cells are highly arborized cells distributed throughout the gray and white matter and make up approximately 4% of all cells in the adult CNS (30, 31). Given that NG2 cells can differentiate into oligodendrocytes from early brain development through adulthood (30, 32–36), it has become accepted that NG2 cells serve as OPCs, even in the adult brain (37). However, not all NG2 cells differentiate into OLs, as large populations persist in gray and white matter areas, a subset of which receive synaptic input from neurons (38, 39) or interact with nodes of Ranvier (40). In response to this neuronal input, these white and gray matter NG2 cells generate action potentials (41), leading to the suggestion that the NG2 cells may be involved in regulating neuronal circuits. These observations have led to the recognition of NG2 cells as a unique glial element, also referred to as synantocytes (42) or polydendrocytes (29, 43).

We have recently reported that NG2$^+$ cells are targets for neurovirulent and nonneurovirulent viruses in the developing brain (10, 44) and that NG2 cell infection by the neurovirulent virus FrCasE is temporally and spatially associated with hyperactivity and functional loss in neurons that fire action potentials after hyperpolarization (i.e., rebound neurons) (44). However, the specific role NG2 cell infection plays in pathogenesis remains unclear, as their infection with the neurovirulent amphotropic virus 4070A was not sufficient to induce neuronal or glial pathology unless the 4070A virus tropism was expanded by ecotropic Env protein pseudotyping (10). These findings suggested that OPC infection alone is not sufficient to cause neurodegeneration but requires virus expression in other or additional neural cell types to cause disease. How infection of NG2 cells affects them directly and impacts the development of CNS disease is not known.

To formally address whether MLV infection is selectively toxic to OLs or OPCs, interferes with OL differentiation, and/or contributes to spongiform neurodegeneration, we explored several complementary *in vivo*, *in vitro*, and brain chimera approaches where progenitor cell infection and differentiation could be readily followed. Here, we show that NG2 cells/OPCs are major targets of ecotropic MLVs, but we find virus sparingly expressed in mature oligodendrocytes. We find that NG2$^+$ Olig2$^+$ neural progenitor cells (NPCs) can be productively infected in culture by both neurovirulent and nonneurovirulent MLVs (FrCasE and Fr57E, respectively) without apparent cytotoxicity, despite evidence that OPCs were dying *in vivo*. Furthermore, transplantation analysis of *ex vivo*-infected NPCs showed that both FrCasE and Fr57E interfered with their differentiation toward OLs but had no apparent effect on NPC engraftment and persistence. Altogether, the present study provides evidence that NG2 cells/OPCs are major targets of ecotropic MLVs and that this infection interferes with their differentiation toward oligodendrocytes, which in the face of ongoing excitotoxicity likely contributes to viral neuropathogenesis.

MATERIALS AND METHODS

Mice. All animal procedures were performed in accordance with the regulations of the Institutional Animal Care and Use Committee at the Northeast Ohio Medical University and the guidelines of the National Institutes of Health. The mouse strains employed included Inbred Rocky Mountain White (IRW) mice; PLP-EGFP IRW mice, which express cytoplasmic enhanced green fluorescent protein (EGFP) from the myelin proteolipid protein (PLP) promoter that identifies mature oligodendroglia; and *Gt(ROSA)26Sor*$^{tm4(ACTB-tdTomato,-EGFP)Luo}$/J mice (referred to as mTmG mice here), a reporter strain of mice on the 129X1/SvJ background that constitutively expresses membrane-associated TdTomato fluorescent protein (mTomato [mTom]) from the beta-actin promoter in all cells (45). Mice of both sexes were used for virus infection and generation of NPCs and as transplant recipients. Both IRW and 129X1/SvJ mice are highly susceptible to infection and neurodegeneration induced by neurovirulent ecotropic MLVs, while C57BL6 mice are resistant to MLV neurodegeneration (references 5 and 46 and unpublished observations). Because the PLP-EGFP transgene was originally maintained in C57BL6 strain mice (47, 48), it was bred into the IRW background for 10 generations prior to initiation of these experiments. No differences were noted between IRW mice and PLP IRW mice with regard to the onset or severity of FrCasE-induced disease (unpublished observation). PLP IRW mice were not examined for differences in susceptibility to Fr57E-induced leukemia or hemolytic anemia.

Virus, virus infection, and virus titration. FrCasE and Fr57E virus stocks were prepared in NIH 3T3 fibroblasts, yielding stocks of 1×10^6 to 2×10^6 focus-forming units (FFU) per ml of tissue culture medium (Dulbecco's modified Eagle's medium [DMEM] supplemented with 10% fetal bovine serum, 2 mM L-glutamine, penicillin [50 IU/ml], and streptomycin [50 μg/ml]). Virus infection of NPCs is outlined below. IRW and PLP-EGFP IRW mice were inoculated intraperitoneally on the day of birth (P0 [<24 h postparturition]) with 2×10^4 to 5×10^4 infectious FrCasE (5) or Fr57E (49) virions or were not inoculated. Animals were euthanized at various time points between 13 and 18 days postinfection (dpi); serum was collected for virus titration analysis, and brains were

collected for histological and immunohistochemical assessment. The mice were examined for cellular virus expression and histological changes between 13 and 18 dpi, a time frame within which vacuolar pathology is well developed, viral protein levels peak, and clinical neurological disease onset occurs in FrCasE-infected mice (50). Virus titers in serum and culture supernatants were determined using a virus titration assay carried out on NIH 3T3 fibroblasts or dunni fibroblasts as described by Czub et al. (12).

NPC culture. NPCs were isolated from P0-to-P2 PLP-EGFP IRW or IRW × mTmG F1 cross mouse brains by using a Neural Tissue Dissociation kit (Papain) following the manufacturer's instructions (Miltenyi Biotec). Isolated neural cells were cultured as neural spheres (NPHs) in DMEM–F-12 (Invitrogen) supplemented with B27 (Invitrogen, Gibco) and 10 ng/ml epidermal growth factor (EGF) (Sigma). NPHs were dissociated chemically by using the mouse NeuroCult Chemical Dissociation kit (StemCell Technologies) and passed every 3 to 4 days. NPCs were infected with FrCasE and Fr57E stocks made from NIH 3T3 cells. To infect NPCs, we employed spinoculation on freshly dissociated cells (51). Briefly, 2 ml of virus stock was spun in TC-6 plates (Nunc) for 2 h at 1,600 × *g* (4°C), and then NPCs, which were passed twice after initial isolation and growth as NPHs, were seeded into the plate. The cells were cultured at 37°C for 3 to 4 h, collected, washed once with phosphate-buffered saline (PBS), and then cultured in EGF-containing NPH medium.

Neural transplantation. For NPC transplantation studies, infected or uninfected PLP-EGFP or mTmG NPCs were chemically dissociated, washed with PBS once, and then resuspended in PBS containing 1% trypan blue at a concentration of ~4×10^4 to 5×10^4 viable cells per μl. The NPC suspensions were injected at 3 positions bilaterally in the brainstem (total, 6; 1 μl each) from the midbrain to the medulla in neonatal IRW mice, as previously reported (52, 53). The brains were collected and analyzed 7 and 14 days posttransplantation (dpt). For transplantation studies using mTomato-expressing NPCs, P0 mouse pups arising from IRW × mTmG crosses (F1) were used for isolation, culture, infection, and transplantation into recipient IRW mice.

NPC-transplanted and virus-infected experimental mice were observed daily for overt signs of disease beginning at P10, a time at which spongiform changes can first be detected within the CNS (50). Clinical neurological signs, including unkempt fur, wasting (body weight less than 80% of age-matched, uninfected controls), kyphosis, tremor, hind- and or forelimb adduction upon elevation by the tail, imbalance, and/or paralysis, were not observed until 15 to 16 dpi, consistent with previous reports for the FrCasE virus (5).

Immunohistochemistry, fluorescence, and histology on cells and tissues. To characterize virus infection and phenotypic changes in NPCs, NPHs, or cells freshly dissociated from them, were seeded onto poly-D-lysine-coated plates and cultured in DMEM–F-12–B27–EGF medium for 3 to 5 h at 37°C for cell attachment. The cells were fixed with 4% paraformaldehyde at room temperature (RT) for 10 min, washed with PBS, and then permeabilized by incubation in PBS containing 0.1% Triton X-100 at room temperature for another 10 min. After blocking with 3% bovine serum albumin (BSA) at room temperature for 20 min, the cells were incubated with the primary antibodies (see below) at the indicated concentrations at room temperature for 1 h and washed with PBS, followed by incubation with fluorescent secondary antibodies for another hour. The cells were washed, coverslipped, and viewed using an Olympus FV-300 confocal microscope.

To assess CNS viral infection and engraftment of NPCs, brains were immersion fixed in 10% buffered formalin and either paraffin embedded or sectioned on a vibratome. For histology or immunohistochemistry, 6-μm paraffin sections were collected, deparaffinized, and either subjected to antigen retrieval before immunostaining or stained with hematoxylin and eosin. For counting transplanted cells expressing transgenic fluorescent proteins (XFPs), fixed brains were cut into 50-μm sections from the forebrain though the medulla, mounted on slides in PBS, and then viewed by epifluorescence. Selected sections with XFP-positive cells were also immunostained for Env protein expression and cell-type-specific markers. To accomplish the immunostaining, free-floating sections were treated with 1% Triton X-100 at room temperature for 30 min and then with avidin/biotin blocking reagent (Vector). Floating sections were incubated with 3% BSA at room temperature for 30 min and then with the primary antibodies at room temperature for 1 h, followed by biotinylated antibodies at RT for 1 h and streptavidin Alexa Fluor 488 or 594 (1:1,000; Invitrogen) at RT for 30 min. CasBrE Env staining with the mouse monoclonal antibody 697 was carried out by using a M.O.M. kit from Vector.

Paraffin-embedded sections were deparaffinized, rehydrated, and then subjected to antigen retrieval in citrate buffer (10 mM sodium citrate, 0.05% Tween 20, pH. 6.0) with autoclaving at 110°C for 10 min (Napco autoclave, model 8000-DSE). Double immunofluorescence staining on paraffin-embedded sections was performed sequentially. The paraffin-embedded sections were incubated with the primary antibodies and then with Alexa Fluor secondary antibodies.

The primary antibodies used in the present study included rabbit anti-NG2 proteoglycan (1:100; Chemincon), rabbit anti-PDGFRα (1:300; Santa Cruz), rabbit anti-Olig2 (1:500; Chemicon), mouse anti-nestin (1:500; Pharmingen), rabbit anti-Iba-1 (1:500; Wako), mouse anti-2′,3′-cyclic nucleotide 3′-phosphodiesterase (CNPase) (1:500; Chemicon), rabbit anti-carbonic anhydrase II (CAII) (1:4,000; Chemicon), mouse anti-PLP (a generous gift from Bruce Trapp, Cleveland Clinic), mouse anti-HuC/D (1:500; Invitrogen), rabbit anti-glial fibrillary acidic protein (GFAP) (1:2,000; Dako), mouse anti-CasBrE Env monoclonal antibody 697 (54), and goat anti-Friend Env serum (1:5,000). The secondary antibodies included anti-mouse, anti-rabbit, and anti-goat Alexa Fluor 555, 488, or 647 (1:1,000; Invitrogen), biotinylated donkey anti-goat IgG, biotinylated donkey anti-rabbit IgG (1:500; Jackson Immunology Research), and biotinylated goat anti-mouse IgG. Images were taken using an Olympus FV-300 confocal microscope. Marker colocalization within individual cells was determined by superimposing z-stack images.

Analysis of EGFP$^+$ and mTomato$^+$ cells. The animals that received retrovirus-infected and mock-infected PLP-EGFP NPCs or mTmG NPCs were perfused with ice-cold PBS, 4% paraformaldehyde, and then the brains were collected and immersion fixed in 4% paraformaldehyde at 4°C overnight and stored in PBS at 4°C. Coronal sections (50 μm) of entire brains, beginning caudal to the vestibular nuclei up to the olfactory bulb, were cut on a vibratome and stored in PBS at 4°C. EGFP- and mTomato-positive cells in transplanted mice were counted by individuals blinded to the infection status of the NPCs. Counting was performed under low-power magnification (100 to 200×) using epifluorescence illumination. For PLP-EGFP NPCs, myelinating and nonmyelinatying cells were counted based on their morphology. EGFP$^+$ cells exhibiting multiple parallel processes were counted as mature myelinating oligodendrocytes. All the other EGFP$^+$ cells were counted as nonmyelinating oligodendrocytes. For brains transplanted with mTomato NPCs, cells were characterized as possessing differentiated versus undifferentiated morphologies. Differentiated cells included cells with more than 3 branched cellular processes extending at least one cell body length from the soma. Morphologies ranged from cells with dense fine processes and blood vessel endfeet, to myelinating cells, to cells with long (>2 cell body lengths) extensively branched processes consistent with NG2 cells. Undifferentiated cells included cells with a rounded, amoeboid, amorphous, or bipolar shape and cells with few extended processes.

Immunoblotting. To examine virus infection and expression of oligodendrocyte differentiation in cultured NPCs, control and MLV-infected NPC spheres were lysed using 0.1% Triton X-100-containing lysis buffer (150 mM NaCl, 50 mM Tris-HCl, pH 7.4, 1 mM $MgCl_2$, 50 mM Pefabloc, and 0.2 mM phenylmethylsulfonyl fluoride [PMSF]) (53) and then centrifuged at 16,000 × *g*, 4°C for 5 min. The supernatants were boiled in sodium dodecyl sulfate-polyacrylamide gel electrophoresis (SDS-PAGE) sample buffer, and proteins were separated by 9% SDS-PAGE, transferred onto polyvinylidene difluoride (PVDF) membranes,

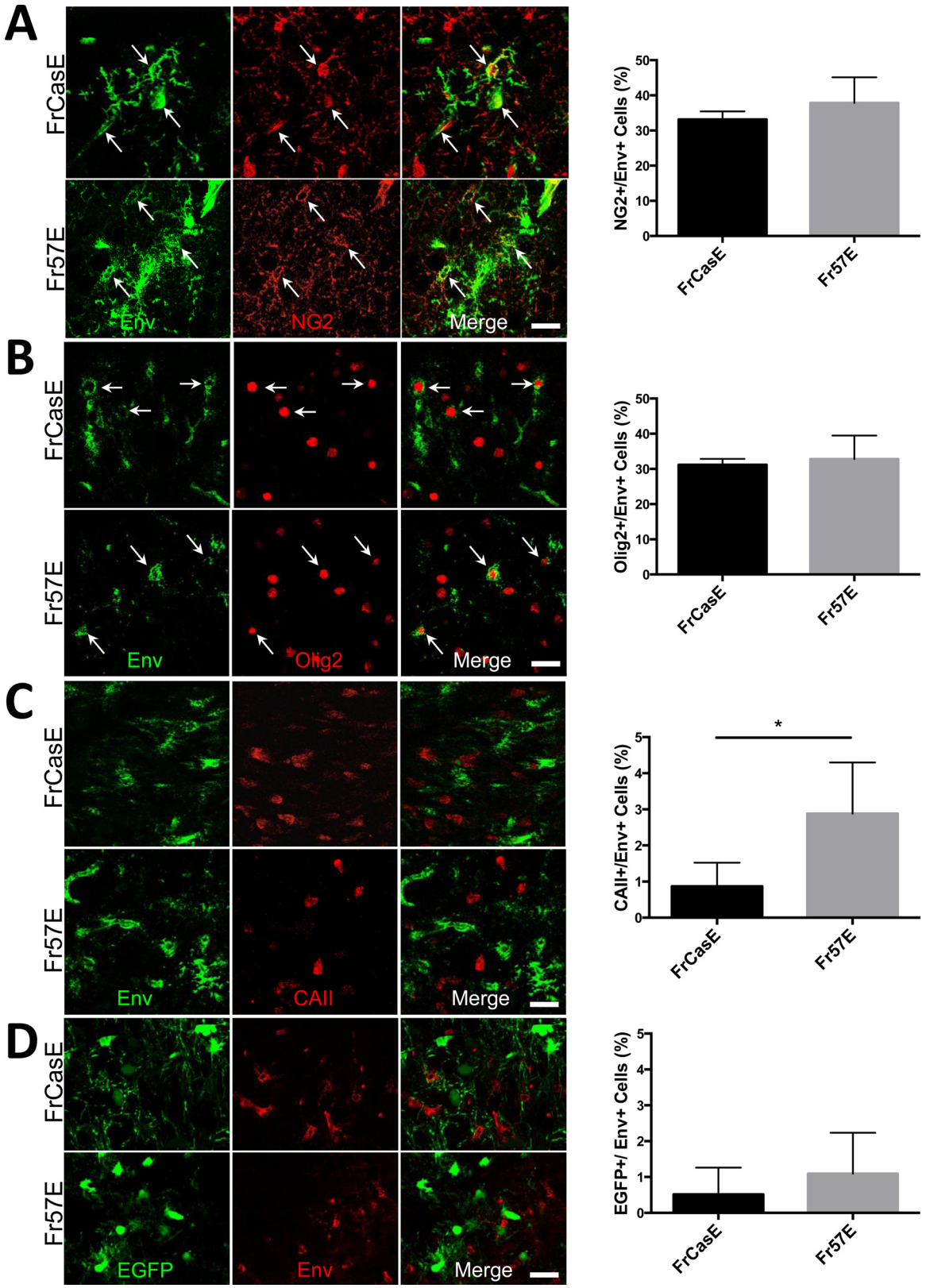

FIG 1 The neurovirulent and nonneurovirulent ecotropic viruses FrCasE and Fr57E, respectively, are expressed in NG2/OPCs, but not in mature OLs. Newborn mice were infected intraperitoneally with FrCasE or Fr57E, and their brains were analyzed by confocal immunofluorescence microscopy for early and late oligodendroglial markers and virus expression between 13 and 18 dpi. (A) Staining for the OPC marker NG2 (red) and FrCasE or Friend 57 virus Env protein (green). The arrows indicate examples of the cellular colocalization of virus and NG2 in the brainstem. The frequency of Env^+ cells expressing NG2 was quantitated and expressed as a percentage of the total number of Env^+ cells detected (FrCasE, $n = 916$ cells from ≥3 brains; Fr57E, $n = 498$ cells from ≥3 brains;

and subjected to immunoblotting for Env protein, GFAP, and the oligodendroglial markers CAII, PLP, and CNPase. The retroviral Envs were detected by goat anti-Friend Env serum, which has cross-reactivity to CasBrE Env. EGFP expression was detected by rabbit anti-EGFP (1:2,000; Abcam) and β-actin by a mouse anti-β-actin IgG (1:1,000; Sigma). The membrane was blocked with 5% nonfat milk and then incubated overnight with primary antibodies diluted in PBS containing 2% bovine serum albumin. The blots were treated with species-specific secondary antibodies coupled to horseradish peroxidase for 2 h, washed, and then developed using chemiluminescent substrate (SuperSignal West Pico chemiluminescent substrate; Pierce). Three separate NPH preparations were analyzed by immunoblotting, and representative examples are shown.

RESULTS

Neurovirulent and nonneurovirulent ecotropic MLVs efficiently infect CNS OPCs, but viral expression in OLs is infrequent. We have recently reported that the neurovirulent and nonneurovirulent ecotropic viruses FrCasE and Fr57E, respectively, infect glial cells in the inferior colliculus (IC) that express the chondroitin sulfate proteoglycan NG2, coincident with the alteration of rebound neuron physiology and spongiogenesis in that brain region (44). Because motor signs, such as tremor and paralysis, are a prominent clinical feature of neurovirulent-MLV-induced spongiosis, we extended our analysis here to include brainstem regions more directly involved in the loss of motor function. As shown in Fig. 1A, colocalization of NG2 proteoglycan and CasBrE and Fr57E Envs was observed to colocalize in ramified extravascular cells in the pons, medulla, cerebellum, and thalamus when examined 14 to 16 dpi. NG2 cells accounted for 33.2% ± 2.3% and 37.8% ± 7.3% of Env^+ cells for FrCasE and Fr57E, respectively. In addition, NG2 cell infection was observed in gray matter areas in the cerebral cortex, striatum, and hippocampus, as well as in the white matter of the corpus callosum, brain areas where spongiform pathology does not typically arise (50).

Since the majority of embryonic and adult NG2 cells express Olig2, a basic helix-loop-helix transcription factor required for oligodendrocyte specification (26), we examined whether FrCasE and Fr57E Env expression colocalized with Olig2 in brainstem sections. As shown in Fig. 1B, Env^+ $Olig2^+$ cells were readily observed, with a frequency similar to that observed for Env^+ $NG2^+$ cells. These findings are consistent with the idea that OPCs are major targets of ecotropic MLVs with the potential to influence neurodegeneration, based on the nature of the Env protein they express.

To evaluate the extent to which ecotropic virus infection could be detected in mature oligodendroglia, we examined infected brainstems for Env expression coincident with the expression of CAII. As illustrated by the example in Fig. 1C and the quantitative assessment, few Env^+ $CAII^+$ cells were observed in either FrCasE- or Fr57E-infected animals sacrificed between 14 and 18 dpi. Interestingly, the frequency of Env colocalization with CAII was significantly higher in Fr57E- versus FrCasE-infected brainstems but was still quite low at ~3%. Whether this difference in virus-expressing OLs was reflective of the ongoing neurodegeneration occurring in the FrCasE-infected mice or instead represents differences in the capacities of the two viruses to interfere with OPC differentiation could not be resolved by this analysis, but we attempt to address it below.

As an independent means to examine virus expression in mature OLs, we examined cellular infection in transgenic mice that express EGFP from the myelin proteolipid protein promoter (PLP-EGFP mice). In these mice, migrating gray and white OLs express high levels of EGFP (EFGP-high) (47). In addition, certain brainstem neurons express much lower levels of EGFP (EGFP-low), allowing the two EGFP populations to be distinguished from one another (Fig. 2E to G) (55). Moreover, this differential expression facilitated a coincident morphological assessment of OLs and vulnerable neurons. As indicated by the example in Fig. 1D, viral Env and EGFP colocalization was not typically observed, and when it was seen, it occurred only in $EGFP^{high}$-expressing cells (as defined above and illustrated in Fig. 2E to G). Unlike CAII and Env colocalization, there was no significant difference in the frequencies of Env colocalization with EGFP between FrCasE- and Fr57E-infected brainstems. Importantly, there were no obvious qualitative changes in the morphology of $EGFP^{high}$-expressing cells in mice infected with FrCasE versus mock- and Fr57E-infected animals, consistent with previous reports assessing oligodendroglial integrity associated with neurovirulent MLV infection of the CNS (16).

OPC infection by ecotropic MLVs in the brainstem is variably associated with spongiform neuropathology. To assess the spatial relationship between virus-infected NG2 cells and spongiform neuropathology, paraffin sections from 14- to 16-dpi FrCasE-infected mouse brainstems were subjected to double-label immunohistochemical analysis for Env and NG2, combined with differential interference contrast microscopy. As illustrated by the examples taken from the pons shown in Fig. 2A and B, we observed that the FrCasE-Env-expressing NG2 cells (black arrows) were often associated with spongiosis (white arrows), with the NG2 cell processes in close apposition to small vacuoles (white arrowheads). However, within the same sections, we also observed areas of spongiosis where Env expression in NG2 cells was not obvious (Fig. 2C, white arrows) and areas without spongiosis but with NG2 cell infection (Fig. 2D, black arrows), making it unclear whether the infection of the NG2 cells by FrCasE was obligatory for spongiogenesis or simply a coincidence. Rarely, $NG2^+$ Env^+ cells could be observed to exhibit vacuolar changes characterized by cytoplasmic effacement, but this was not a prominent feature.

Because it has been reported that OLs are a major target of the toxicity mediated by MLVs (19), we extended our histological examination to FrCasE-infected PLP-EGFP mice using confocal

$P = 0.35$, not significant). (B) Staining for the OPC nuclear transcription factor Olig2 (red) and Env (green); the arrows indicate Env^+ Olig2-positive cells. The graph (right) shows the frequency (expressed as a percentage) of Env^+ cells expressing Olig2 (FrCasE, $n = 409$ cells from ≥4 brains; Fr57E, 697 cells from ≥3 brains; $P = 0.64$, not significant). (C) Staining for the mature OL marker carbonic anhydrase II (red) and viral Envs (green), where no colocalization was noted, indicative of the low frequency of Env^+ cells that also stained for CAII, as shown in the graph. Note that there was a significant difference (*, $P < 0.05$) between the frequencies of detecting FrCasE Env and Fr57E (FrCasE, $n = 377$ cells from ≥4 brains; Fr57E, $n = 1{,}416$ cells from ≥5 brains; $P = 0.031$; Student's t test). (D) Immunostaining for viral Envs (red) in PLP-EGFP brainstem sections, where mature OLs expressed high EGFP levels (green). As indicated by the examples and in the graph, the detection frequency of EGFP expression in Env^+ cells was quite low and did not significantly differ between FrCasE and Fr57E (FrCasE, $n = 1{,}302$ cells from ≥5 brains; Fr57E, $n = 1{,}107$ cells from ≥5 brains; $P = 0.37$). The error bars in the graphs represent standard deviations, and all data sets were analyzed by Student's t test. Scale bars, 20 μm.

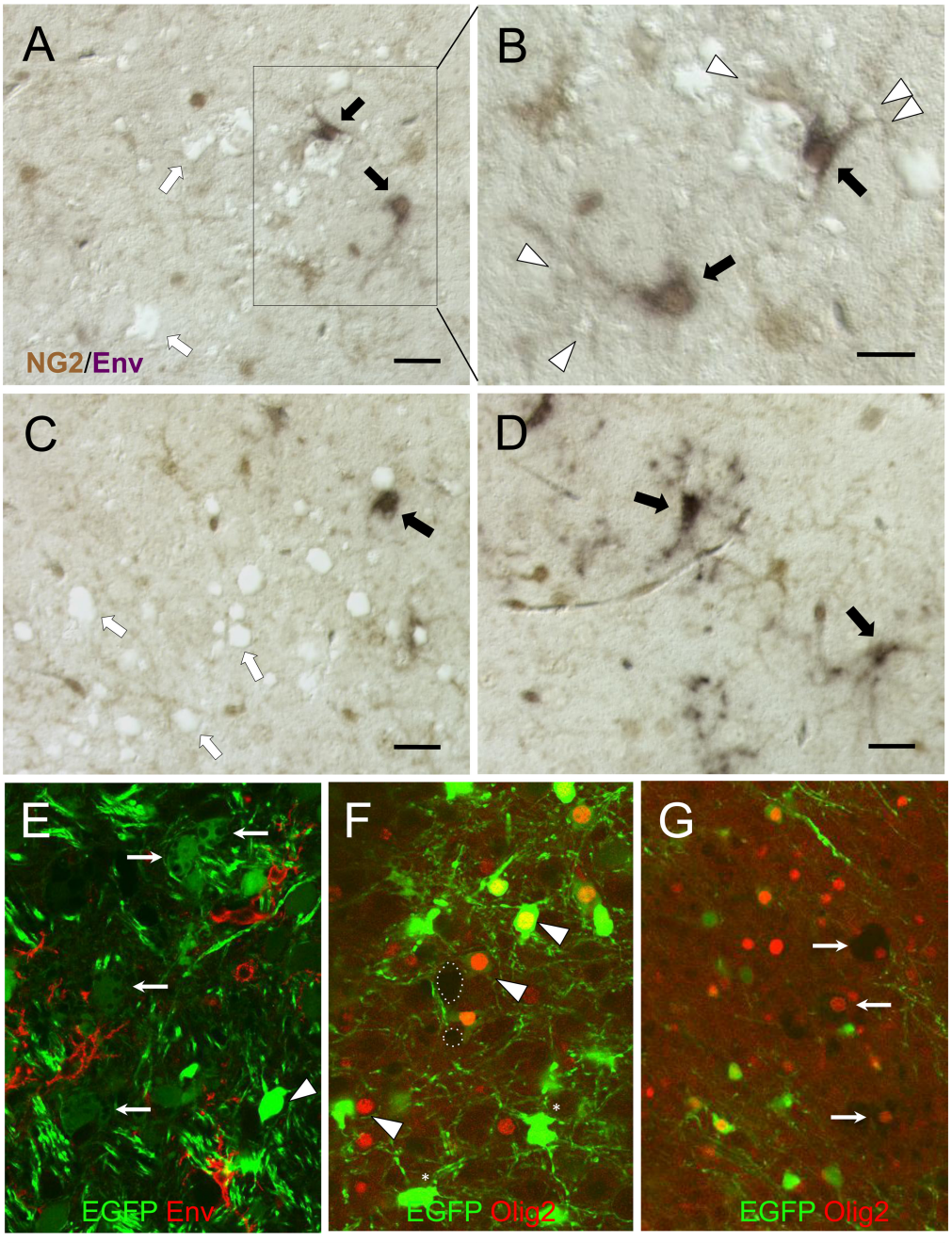

Cell Identification	EGFP-negative	EGFP-low	EGFP-high
Olig2-positive	Early OPC	OPC/neuron(?)	Late OPC/OL
Olig2-negative	Non OL lineage cell	Neuron	Mature OL

FIG 2 NG2/OPC infection by FrCasE is variably associated with spongiform neurodegeneration. (A to D) Representative examples of paraffin sections from the brainstems of FrCasE mice at 15 dpi double immunostained for Env (purple) and NG2 (brown) and viewed using differential interference contrast (DIC) optics to simultaneously visualize vacuolar changes without the need for a tissue counterstain. (A to C) Examples of $NG2^+$ Env^+ cells (black arrows) in close association with both small (arrowhead) and large vacuoles. In addition, vacuolation is seen without clear association with $NG2^+$ Env^+ cells (white arrows). (D) $NG2^+$ Env^+ cells can also be observed in brainstem regions without vacuolation. (E to G) Representative confocal examples from thick sections showing spongiform changes in the brainstems of FrCasE-infected PLP-EGFP transgenic mice at 15 dpi. At the bottom is a table for interpreting the cell identities based on EGFP expression (green) and Olig2 nuclear immunostaining (red). (E) Relationship of viral-Env-expressing cells (red) to appearance of cell body vacuolation in $EGFP^{low}$ cells (arrows) but not $EGFP^{high}$ cells (arrowhead). (F) Example of Olig2 immunostaining in a FrCasE-infected PLP-EGFP brainstem section showing that Olig2 expression (arrowheads) can be observed in $EGFP^{high}$, $EGFP^{low}$, and $EGFP^{neg}$ cells. In addition, $EGFP^{high}$ cells were observed without Olig2 expression (asterisks). Vacuolation (e.g., dotted circles) was rarely observed in $EGFP^+$ $Olig2^+$ cells (not shown), despite the common observation of vacuoles in cells expressing low EGFP levels. (G) Cytoplasmic effacement (a subtype of vacuolar neurodegeneration) occurred predominantly in cells in which the remnant nuclei expressed Olig2 (arrows) but without detectable EGFP. Scale bars, 20 μm.

images from thick sections. Interestingly, when mice were examined between 14 and 16 dpi ($n = 6$ brains), we found no evidence for vacuolation of EGFP^{high}-expressing cells (cf. Fig. 2E to G). In contrast, it was commonplace to see cell body vacuolation in cells that were EGFP^{low} in proximity to Env (red)-expressing cells (Fig. 2E, arrows). The EGFP^{low} cells in PLP-EGFP mice likely represent brainstem neurons, as previously described for these mice (55). We next examined the relationship of Olig2 expression to EGFP expression and cellular vacuolation. As shown in Fig. 2F and G, Olig2 was observed in EGFP^{high}, EGFP^{low}, and EGFP-negative (EGFP^{neg}) cells, but not all EGFP$^+$ cells were positive for Olig2, and only a subpopulation of Olig2$^+$ cells expressed EGFP. Thus, the Olig2 and EGFP markers in PLP-EGFP mice identify overlapping CNS cell populations, with Olig2 identifying OPCs and early OLs and EGFP^{high} identifying early and mature OLs. No apparent differences in Olig2/EGFP colocalization were noted between control ($n = 5$; not shown), FrCasE-infected ($n = 6$), and Fr57E-infected ($n = 3$; not shown) PLP-EGFP mice. Interestingly, in FrCasE-infected PLP-EGFP mice, we failed to observe any EGFP^{low} Olig2$^+$ cells showing cytoplasmic vacuolation, while cells showing severe cytoplasmic effacement were observed to be Olig2$^+$ but EGFP^{neg} (Fig. 2G). Whether these cells were EGFP$^+$ OLs that lost EGFP expression or OPCs that never expressed EGFP could not be determined without a means to trace individual cell fates.

FrCasE and Fr57E infection of NPCs in culture is not cytotoxic but can reduce expression of certain glial differentiation markers in NPHs. We have previously shown that the conditionally immortalized neural stem cell (NSC) line C17.2 can be productively infected by both neurovirulent and nonneurovirulent viruses in culture without cytotoxic effects, either *in vitro* or after their transplantation into developing neonates (reviewed in reference 56). However, C17.2 NSCs have been conditionally immortalized with v-*myc*, which could impact their susceptibility to neurotoxic effects of MLVs. Therefore, to address the possibility that MLV infection of NPCs may affect their viability or glial differentiation potential, we infected NPCs derived from neonatal PLP-EGFP mice with FrCasE and Fr57E under conditions where the NPCs grew as NPHs. As suggested by the representative images of immunostained NPHs in Fig. 3A, MLV exposure did not cause any overt changes in sphere formation or cellular growth during early NPH passages (<10). However, with late passages of FrCasE- or Fr57E-infected NPHs, the cells exhibited slower growth (that is, required less frequent passage) and the NPCs were more prone to attach to the culture plates instead of growing as spheres. Mock-infected NPCs showed continued growth as spheres in suspension through at least 16 passages before growth slowed and/or cell attachment became noticeable. Immunostaining of spheres for viral-protein expression and stem cell and glial progenitor cell markers did not show notable differences in expression (Fig. 3A); however, because antibody penetration into fixed NPHs was inconsistent and the resolution of membrane protein expression in adjacent cells in NPHs was challenging, NPC protein expression frequencies were determined by immunostaining single cells from dissociated NPHs after attachment to polylysine-coated slides. The results, summarized in Fig. 3B, showed that approximately 90% of the NPCs exposed to FrCasE or Fr57E expressed detectable levels of Env protein. In addition, immunostaining for the pan-neural stem cell marker nestin was greater than 90%, and more than 95% of the cells expressed the OPC markers NG2, Olig2, and PDGFRα. The frequency analyses suggest that neither FrCasE or Fr57E infection qualitatively or quantitatively affected NG2, Olig2, and PDGFRα expression, which was confirmed by double immunolabeling of cells for the OPC markers and Env. A small but statistically significant increase in the percentage of cells expressing nestin was noted in FrCasE-infected NPCs over mock-infected cells, but no differences were noted between FrCasE- and Fr57E-infected NPCs or mock- and Fr57E-infected NPCs.

Pedraza et al. have reported that some PLP-EGFP NPCs expressed EGFP in NPHs (57), a finding consistent with other studies suggesting that cells within NPHs can express markers of mature glia (cf. reference 58). As can be seen in Fig. 3A, expression of EGFP in a subset of NPH cells was observed in both infected and uninfected NPHs, with the frequency of positive cells varying from one NPH to the next. In surveying the NPH populations in total, EGFP fluorescence intensity appeared to be lower in FrCasE- and Fr57E-infected than in mock-infected NPHs. Because EGFP fluorescence was variable between individual NPHs, we assessed the effect of virus infection on EGFP expression semiquantitatively by Western blotting with antibody to EGFP. As shown in Fig. 3C (left), EGFP protein levels were dramatically decreased relative to actin when NPHs were infected by either FrCasE or Fr57E. To examine whether the virus effect on PLP-EGFP expression in NPCs was cell intrinsic or required cell-cell interaction, NPHs were dissociated, plated on poly-D-lysine, and evaluated for EGFP expression. Interestingly, regardless of whether they were infected, dissociated NPCs showed much lower EGFP fluorescence intensity with no clear difference between controls and CasBrE Env- or Friend Env-positive cells (not shown), suggesting that PLP-EGFP expression was dependent on cell-cell contact or conditions unique to the NPHs. Analysis of attached cells by Western blotting was not undertaken.

To test whether the decreased PLP-EGFP was unique to the transgene or reflected changes occurring more broadly in other OL-specific proteins, we examined the effects of MLV infection of NPHs on CNPase, PLP, and CAII protein expression. These proteins were not detectable by Western blotting in the same NPH samples examined for EGFP, with or without virus infection. However, Western blot analysis for GFAP, an intermediate filament protein marker expressed in most astrocytes and at low levels in NPCs, showed dramatically reduced GFAP expression levels with NPH infection (Fig. 3C). Interestingly, GFAP reduction was greater for the neurovirulent virus, FrCasE, than for the nonneurovirulent Fr57E. This finding suggests that GFAP reduction was a direct result of NPC expression of the neurovirulent Env protein encoded by FrCasE, since the virus is otherwise isogenic to Fr57E.

To assess whether infection of the primary NPCs was permissive for virus replication, supernatants from mock- and MLV-infected NPH cultures were tested for infectious virus after 2 to 5 NPH passages. Figure 3D shows that high titers of infectious FrCasE and Fr57E virus were being produced by these cultures, with no detectable virus production from mock-infected NPCs.

MLV infection restricts OL differentiation in the developing brainstem. Our observation of abundant OPC infection but rare infection of mature OLs has several possible explanations. First, ecotropic MLVs may infect only OPCs that cannot differentiate into OLs. Second, MLV infection may be toxic to OPCs that differentiate into OLs. Third, MLV infection may suppress the markers we employed for OL assessment. Fourth, OL differentiation of

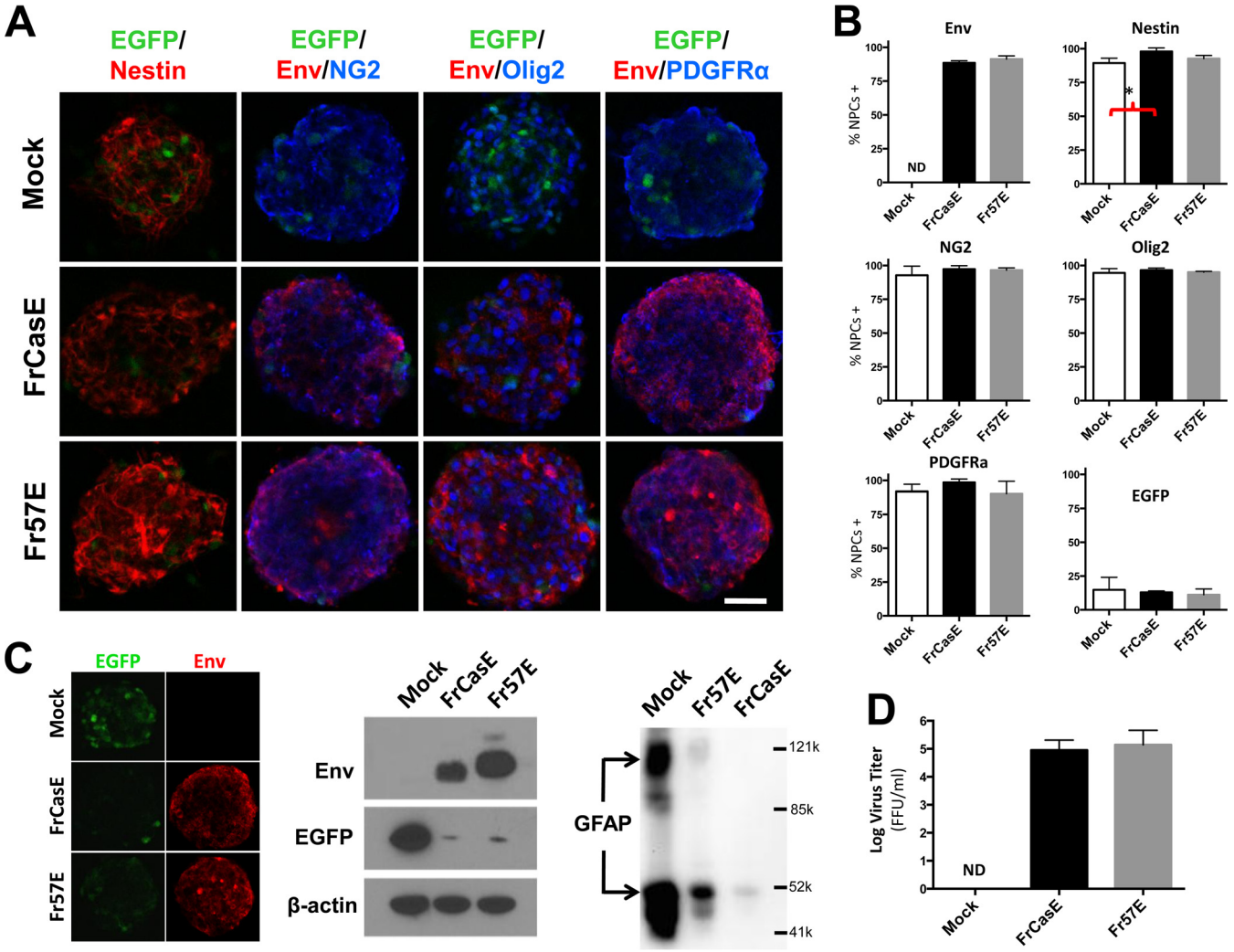

FIG 3 Productive infection of primary NPCs by ecotropic MLVs does not affect neural-sphere formation or OPC marker expression but reduces markers of OL and astrocyte differentiation. (A) Examples of NPHs derived from PLP-EGFP transgenic mice with and without infection with FrCasE or Fr57E virus. These NPHs express low levels of EGFP (green) in a subpopulation of cells within the spheres. NPHs were immunostained for the neural stem cell marker nestin (red, first column on left) or stained for the OPC marker NG2, Olig2, or PDGFRα (blue) and double stained for viral Env protein (red), and images were captured using epifluorescence optics. Scale bar, 50 μm. No gross morphological or immunostaining differences were noted with virus infection, although the intensity of EGFP staining in individual cells appeared lower in the MLV-infected NPHs (cf. panel C). (B) Quantitation of the percentages of cells in the NPH cultures expressing viral Envs and the NPC and OPC markers, which were determined after dissociation of the NPHs into single cells to allow more accurate assessment of individual cell expression. The only significant difference in marker expression frequency was a small increase in the percentage of cells expressing nestin with FrCasE- versus mock-infected NPHs (*, $P = 0.044$; ANOVA). (C) (Left) Nonmerged images of NPHs from panel A (far right column) showing EGFP expression (left; green) and Env staining (right; red), indicative of reduced EGFP expression with virus infection. (Middle) Western blot comparison of FrCasE-, Fr57E-, and mock-infected NPHs probed for MLV Env (top), EGFP (middle), and actin (bottom) showing a dramatic reduction in EGFP expression with MLV infection. (Right) Immunoblotting of NPH extracts with antibody specific for the astrocyte-specific marker GFAP for protein equivalents from mock- and MLV-infected NPHs. Apparent molecular masses are indicated by reference protein sizes listed in daltons. (D) Culture supernatants from NPHs taken after ≥5 passages in culture produced infectious virus when assayed by virus titration assay. Titers are given in FFU/ml. The error bars in the graphs represent standard deviations. ND, not detected. Data sets were analyzed by one-way ANOVA, with Tukey's *post hoc* test for multiple comparisons.

OPCs could suppress virus/Env expression, and thus, we cannot detect infection. Alternatively, MLV infection might interfere with OL differentiation. To explore which, if any, of these possibilities were operating, we employed an NPC-based brain chimera strategy that would allow us to follow the fate of infected OPCs within the developing brain. In the first set of experiments, NPCs were isolated from PLP-EGFP mice infected *ex vivo* with FrCasE or Fr57E as NPHs, and then dissociated NPHs were transplanted into P0 mouse brainstems to follow NPC survival and differentiation. Mice were screened for the presence of $EGFP^+$ cells at 7 and 14 dpt and characterized morphologically. Figure 4A shows examples of the $EGFP^+$ myelinating and nonmyelinating phenotypes that were observed at both the early and late time points. Myelinating cells were characterized by the presence of multiple parallel myelinating processes (arrows), while the nonmyelinating cells were characterized by arborized or spindle-shaped cells whose processes were more restricted (arrowhead and inset). Quantitative comparison of $EGFP^+$ cells in mock-, FrCasE-, and Fr57E-

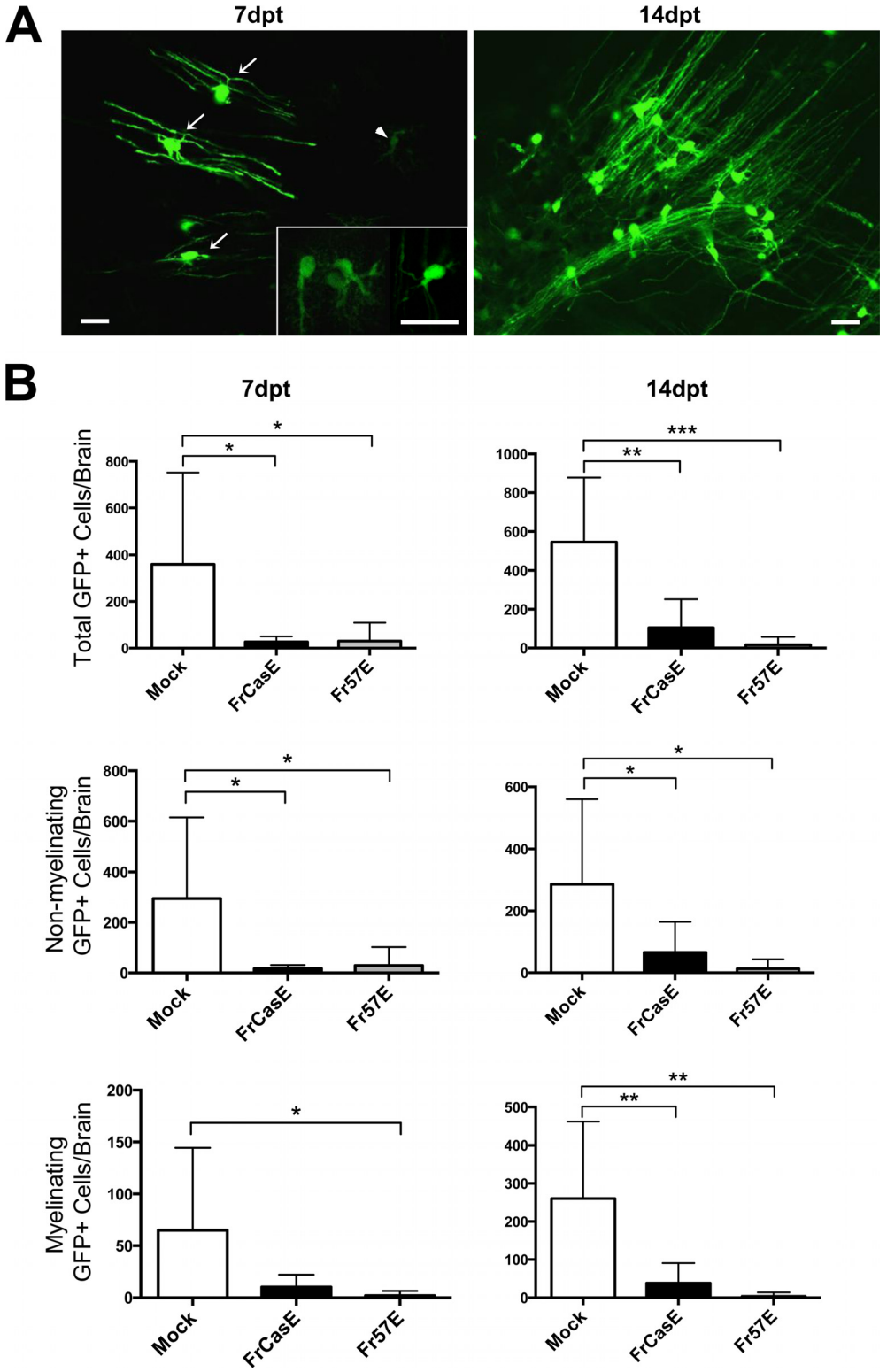

FIG 4 Ecotropic MLV infection interferes with the differentiation of OPCs into mature OLs. *Ex vivo*-infected PLP-EGFP NPHs were dissociated, and the cells were transplanted into P0 IRW mouse brainstems that were subsequently assessed for EGFP-expressing cells at 7 and 14 dpt. (A) Representative epifluorescent examples of $EGFP^+$ cells in 50-μm-thick sections with myelinating (arrows) and nonmyelinating (arrowhead and inset) morphologies that were readily observed in mice receiving mock-infected NPCs but were less frequently observed in mice transplanted with MLV-infected NPCs (scale bars, 20 μm). (B) Quantitative assessment of engrafted cells expressing EGFP at 7 and 14 dpt for total $EGFP^+$ cells, nonmyelinating $EGFP^+$ cells, and myelinating $EGFP^+$ cells. The error bars in the graphs represent standard deviations. Statistical differences were determined by one-way ANOVA, with Tukey's multiple-comparison test. *, $0.01 < P \leq 0.05$; **, $0.001 < P \leq 0.01$; ***, $P \leq 0.001$. Mock, $n = 7$ brains; FrCasE, $n = 8$ brains; Fr57E, $n = 7$ brains. Note that the y axis scale varies for each graph.

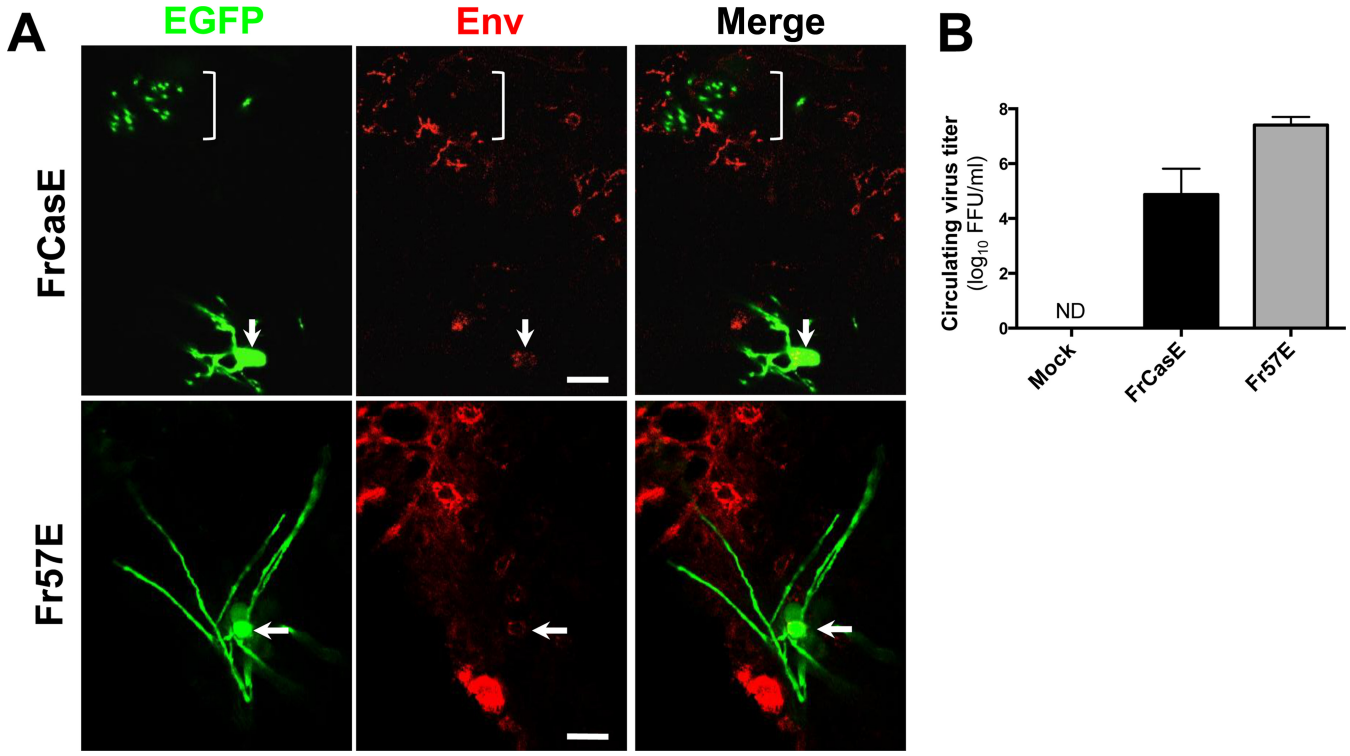

FIG 5 Brainstem transplantation of MLV-infected primary NPCs results in suppressed Env expression in cells differentiating into OLs but generates high circulating virus titers. (A) Confocal images indicating the nature of immunostaining for viral Env (red) associated with engrafted FrCasE- and Fr57E-infected PLP-EGFP NPCs expressing high levels of EGFP. Note that the myelinating processes, imaged perpendicular to the axons (top, bracket) for FrCasE, and along their length for Fr57E, fail to show colocalization of Env and EGFP, while the cell bodies show barely detectable levels of Env expression (arrows). Note that other CNS cells show readily detectable Env expression (red) for both viruses, suggesting that virus expression was cell type restricted. Scale bars, 10 μm. (B) Circulating peripheral virus titers in recipient mice at 14 dpt of virus-infected NPCs, as determined by virus titration assay of the serum. Titers are given in FFU/ml. The error bars indicate standard deviations. ND, not detected.

infected NPC-transplanted mice (Fig. 4B) indicated that FrCasE and Fr57E infection significantly reduced the numbers of EGFP$^+$ cells that could be detected at 7 and 14 dpt. The difference in EGFP$^+$ cells with a myelinating phenotype was not significant between mock and FrCasE infections at 7 dpt but was significant between mock and Fr57Einfections. However, the difference in the number of EGFP$^+$ myelinating cells was highly significant for both FrCasE and Fr57E compared to mock infection when assessed at 14 dpt, a developmental time when OL maturation dramatically increases. The numbers of nonmylinating EGFP$^+$ cells were significantly lower than those of mock-infected cells for both FrCasE and Fr57E transplants at both 7 and 14 dpt.

To assess transplanted cells for persistent virus expression upon engraftment and differentiation, a small number of EGFP$^+$ sections were immunostained for FrCasE and Fr57E viral Env protein colocalization with EGFP (Fig. 5A). In Fr57E-PLP-EGFP NPC-transplanted brains, 14/136 EGFP$^+$ cells (2/12 myelinating and 12/124 nonmyelinating) were weakly positive for Friend Env. EGFP expression was noted to be very low in the Env$^+$ nonmyelinating cells, consistent with an immature phenotype and/or EGFP downregulation, as noted in the infected NPH cultures. In FrCasE-PLP-EGFP NPC-inoculated brains, only 2/162 EGFP$^+$ cells (1/85 myelinating and 1/77 nonmyelinating) were found to express CasBrE Env, albeit weakly compared to other infected cells in the same sections. The low apparent frequency of Env$^+$ EGFP$^+$ cells parallels the results shown in Fig. 1 for Env expression in mature OLs in wild-type and PLP-EGFP transgenic mouse brains. These results suggest that transplanted cells with high MLV expression died, suppressed EGFP expression, or failed to differentiate. Alternatively, MLV expression itself may have been suppressed as the OPCs differentiated into OLs. Nonetheless, virus expression from the transplanted NPCs resulted in virus spread within the brain parenchyma (Fig. 5) and high circulating virus titers (Fig. 5B) and induced spongiosis in mice transplanted with FrCasE NPCs (not shown).

Ecotropic MLV-infected NPCs engraft, persist, and differentiate in the developing brainstem. Given that the number of EGFP$^+$ cells found in brains transplanted with FrCasE- and Fr57E-infected PLP-EGFP NPCs was significantly lower than that in mock-infected NPCs, it was not clear whether the transplanted NPCs failed to survive, persisted as progenitors, or differentiated into non-OL cell types. Therefore, to more directly follow the fate of the transplanted progenitors with infection, NPCs were derived from an F1 cross between IRW mice and mTmG transgenic mice. All the cells in these mice constitutively express the membrane-targeted tdTomato fluorescent protein (mTom) regardless of their differentiation state (45). As shown in Fig. 6A, mice transplanted with infected and uninfected mTom NPCs showed that both control and MLV-infected NPCs engrafted, migrated, and persisted in the brainstems when examined at 7 and 14 dpt.

Quantitative assessment of mTom$^+$ NPC engraftment (Fig. 6B) indicated that there were no significant differences between

control, FrCasE-infected, and Fr57E-infected NPCs at 7 dpt. Interestingly, we observed a substantial elevation in the number of engrafted mTom$^+$ cells in FrCasE-infected NPC transplants compared to controls or Fr57E-infected NPCs at 14 dpt but no difference between control and Fr57E-infected NPC transplants. No evidence of abnormal cellular morphologies or vacuolation was observed with or without virus infection, suggesting that FrCasE or Fr57E was not overtly cytotoxic to NPCs in the *in vivo* setting. The increase in mTom$^+$ cells observed with FrCasE-infected NPCs at the 14-dpt time point suggests that the NPCs proliferated after transplant. Because FrCasE NPCs disseminate virus and precipitate spongiosis, the simplest explanation for their expansion was that they responded to the neurodegeneration that initiates once the CNS has developed past P10 (59) rather than to proliferative effects of virus infection itself. While the assumption is that the transplanted NPCs reflect processes occurring in endogenous progenitor cells, more detailed testing will be required to confirm that NG2 cell proliferation is a feature inherent in virus-induced neurodegenerative diseases.

Morphologically, the mTom$^+$ cells appeared either as undifferentiated, amorphous cells with few or limited processes (Fig. 6A, asterisks), similar to the nonmyelinating phenotypes shown for PLP-EGFP NPCs, or assumed highly ramified morphologies, consistent with the maturation of the NPCs into more mature glial phenotypes. The complexity of the cellular processes was noted to be more elaborate at 14 dpt versus 7 dpt, suggestive of ongoing cellular differentiation. In particular, many cells were noted to exhibit a very bushy or fibrous appearance with abrupt edges abutting vascular elements characteristic of astrocytes with blood vessel endfeet (Fig. 6A, arrowheads). Immunostaining of brainstem sections from engrafted mice for GFAP suggested that many of these mTom$^+$ cells were astrocytes (Fig. 6C and D). In transplants of control NPCs, we also observed many mTom$^+$ cells with morphologies consistent with myelinating oligodendroglia at 14 dpt (Fig. 6A, arrows). In contrast, mTom$^+$ myelinating cells were rarely detected in mice transplanted with ecotropic virus-infected NPCs, consistent with the idea that ecotropic MLV infection interferes with OPC differentiation into OLs. Interestingly, we did not detect mTom$^+$ cells exhibiting vacuolar pathology in mice transplanted with FrCasE-infected NPCs; however, we did not assess the extent to which these cells integrated as NG2 cells establishing synaptic contacts with susceptible neuron populations.

To assess whether MLV infection influenced NPC differentiation in a general way, the morphology of the engrafted cells for each condition was quantified based on whether the cells possessed any of several differentiated phenotypes or appeared to be undifferentiated (as described above). As shown in Fig. 6B, bottom, no significant differences in the fractions of cells taking on a differentiated phenotype were noted between control and FrCasE NPCs at either 7 or 14 dpt, although there may be a trend toward higher levels of differentiation with FrCasE infection. In contrast, Fr57E NPC differentiation was significantly lower than that of FrCasE NPCs at 7 dpt, which became a very highly significant reduction in differentiation versus both FrCasE-infected and control NPCs by 14 dpt. Which glial population is specifically affected by Fr57E and whether global interference with NPC differentiation impacts why the virus fails to precipitate neurodegeneration are provocative questions worthy of future analysis. Because FrCasE and Fr57E NPCs were shown to be productively infected in culture, the expectation was that these cells would continue to express virus upon transplantation and infect adjacent host glia. Thus, sections from brainstems transplanted with FrCasE and Fr57E NPCs were immunostained for viral Env protein and compared with mTom$^+$ transplanted NPCs at 14 dpt. As shown in Fig. 6D, Env expression was readily apparent in ramified and vascular cells adjacent to the engrafted mTom$^+$ cells. Interestingly, we also noted that Env expression in many of the engrafted mTom$^+$ cells was often quite low, raising the possibility that viral expression was suppressed in certain cells upon differentiation *in vivo*. Immunostaining for GFAP showed that astrocytes constitute at least one mTom$^+$ cell type expressing different levels of Env, with expression most obvious in the perinuclear regions of the cells expressing low levels of Env.

DISCUSSION

In this report, we have examined the consequences of ecotropic MLV infection of NG2 glial cells in order to understand their potential to contribute to the spongiform neurodegeneration associated with various neuropathogenic viruses and abnormal proteins. Our findings indicate that progenitor cells expressing the OPC markers NG2 and Olig2 represent one-third of the viral targets in brain regions that undergo neural vacuolation. Because mature OLs in these regions infrequently express detectable Env, the possibility existed that virus infection was directly cytotoxic or prevented OPC-to-OL differentiation. Conversely, OPC infection followed by OL differentiation could have suppressed virus expression. In considering these possibilities, we confirmed the previous findings of Clase et al. (19), showing that the glial cells undergoing cytoplasmic effacement expressed nuclear Olig2. However, we were unable to identify Olig2$^+$ EGFP^{high} cells showing vacuolar changes in the PLP-EGFP mice infected with FrCasE. These results suggest that glial degeneration occurs at a pre-OL developmental stage, which likely corresponds to the long-term NG2 glia. The vacuolated EFGP^{low} cells we routinely observed in PLP-EGFP mice likely reflect degenerating brainstem neurons, given the lack of Env or Olig2 expression and the previous report by Miller et al. highlighting EGFP^{low} expression in medulla neuron populations in PLP-EGFP transgenic mice (55). Nonetheless, we cannot rule out the possibility that these cells could be FrCasE-infected OLs with suppression of both EGFP and viral Env, since we observed MLV suppression of EGFP in cultured PLP-EGFP NPHs and barely detectable Env expression in the mice engrafted with infected PLP NPCs.

By examining infection of NPCs *ex vivo*, we observed that neither FrCasE nor Fr57E was directly cytotoxic, but rather, both acted to suppress a readout marker for OL differentiation, i.e., PLP-EGFP expression, as well as to suppress GFAP, a marker of astrocyte differentiation. Interestingly, by examining cellular fate/survival via the reintroduction of transgenic NPCs into the developing CNS, virus-associated NPC loss was not observed. In fact, NPC numbers were significantly higher in FrCasE NPC-transplanted mice than in control and Fr57E NPCs at 14 dpt, consistent with the idea that cellular proliferation occurred in response to FrCasE-induced neurodegeneration, rather than to FrCasE infection of the NPCs. A rudimentary morphological assessment of engrafted NPC transition to highly arborized cells indicated that Fr57E, but not FrCasE, infection significantly interfered with this process. Whether the more limited differentiation observed for Fr57E NPCs impacts its neurovirulence is not known, but it is well established that neurodegeneration requires CNS maturation be-

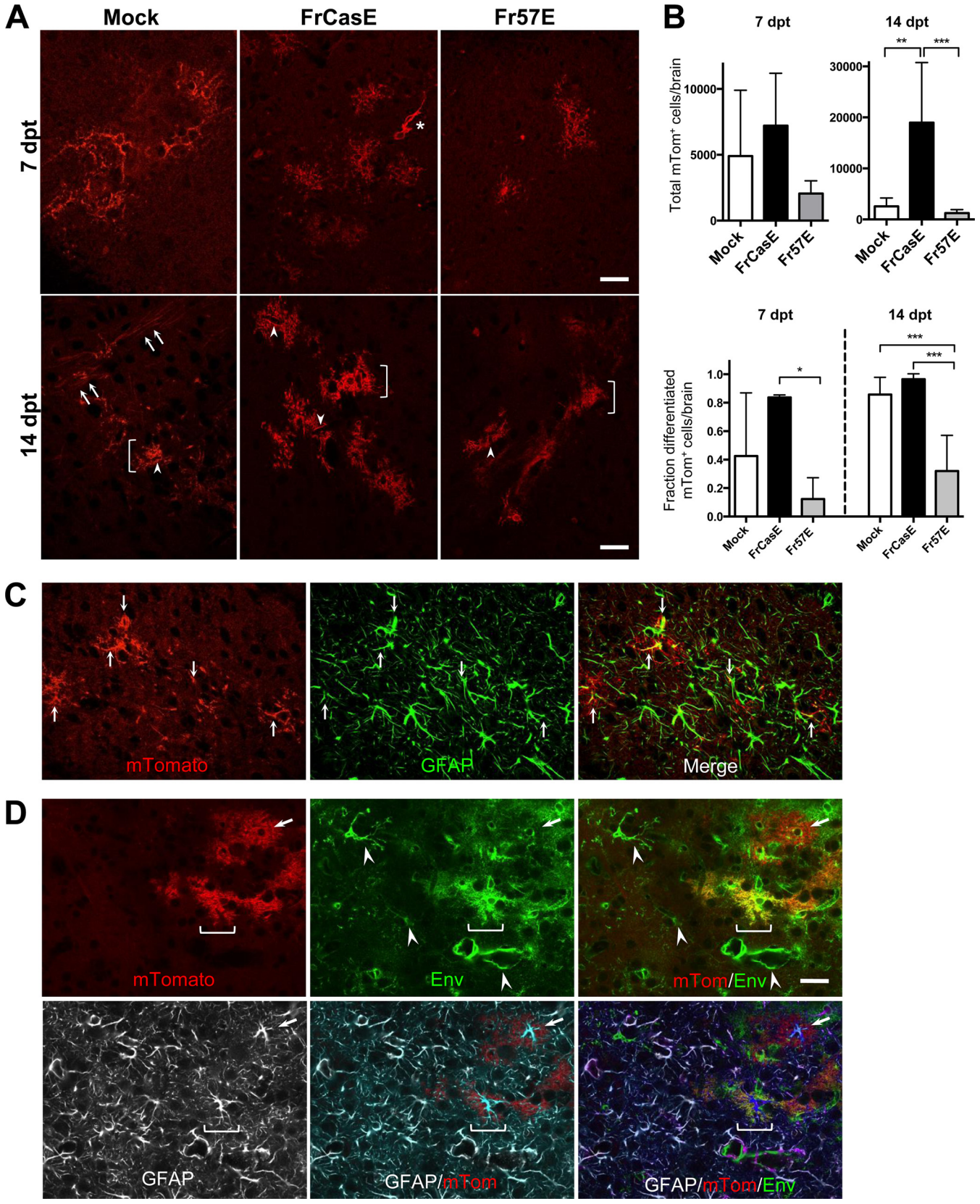

FIG 6 Transplanted MLV-infected primary mTmG NPCs engraft, persist, differentiate into astrocytes, and facilitate virus spread to host cells. (A) Representative examples of $mTom^+$ cells found within the brainstems of IRW mice at 7 and 14 dpt for mock-, FrCasE-, and Fr57E-infected NPCs exhibiting highly arborized morphologies. At 14 dpt, $mTom^+$ cells with morphologies consistent with astrocytes (brackets) could be seen in animals receiving either infected or uninfected

yond the first postnatal week (59). The idea that the CNS developmental requirement may involve the functional maturation of infected glia is interesting; however, our experiments engrafting PLP-EGFP-derived NPCs showed that both viruses interfered with OL differentiation. Our studies also indicated that astrocyte differentiation appeared to be unaffected by either FrCasE or Fr57E, despite the *in vitro* finding that FrCasE most dramatically suppressed GFAP expression in NPHs. This finding suggests that the virus-suppressive effects on astrocyte marker expression were countered by signals present within the developing CNS. However, because the analysis of astrocyte differentiation here was limited in scope, it is not yet known whether FrCasE and/or Fr57E might have differentially affected astrocyte development and/or physiology in ways relevant to neuropathogenesis, as suggested by others (60–62). Nonetheless, we did observe that Env expression in mTom$^+$ astrocytes varied between cells, raising the possibility that virus expression could be suppressed with cellular differentiation. Given that astrocyte virus expression associated with neurodegeneration has only rarely been observed in animals infected with CasBrE-related viruses (14, 20, 22), these findings suggest that a complex interplay between virus and progenitor cell differentiation occurs within the CNS and thus warrants a more comprehensive qualitative and quantitative assessment.

In this study, we observed that that both neurovirulent and nonneurovirulent MLVs were similarly capable of inhibiting OL differentiation, and thus, by itself, this activity cannot account for differences in the induction of spongiform neurodegeneration. Nevertheless, inhibition of OL differentiation might be a critical factor contributing to disease when combined with Env-mediated excitotoxic activities. For example, culture findings show that human endogenous retrovirus W (HERV-W) Env inhibits OPC expression of myelination proteins, and thus, it has been suggested that HERV expression in humans could interfere with OPC remyelination in multiple sclerosis (63). Similarly, human immunodeficiency virus type 1 (HIV-1) and/or Env and Tat proteins have been shown to inhibit NPC proliferation and neurogenesis (reviewed in reference 64), affect Olig2 expression in NPC cultures (65), and bias NPCs toward an astrocytic fate in culture (65, 66). Whether HIV interactions with NPCs contribute to HIV-associated white matter pallor has not yet been investigated. Moreover, recent findings on sporadic amyotrophic lateral sclerosis (ALS) indicate that HERV-K expression occurs at a high frequency in ALS patient brain samples (67) and can induce motor neuron degeneration in transgenic mice (68). In a related familial mutant superoxide dismutase 1 (mSOD-1) ALS mouse model, motor neuron degeneration was shown to be associated with loss of OL neuronal support, demyelination, and OPC proliferation, but the OPCs were incapable of differentiation and remyelination. Removal of mSOD-1 from the OLs in these mice delayed disease onset and prolonged survival (69). Thus, retroviral inhibition of OPC differentiation may play an important role in neurodegenerative diseases, where demyelination is a prominent feature.

In considering how retroviral inhibition of OL differentiation might influence OPC viability within the CNS, studies characterizing the interactions between NG2 glia and neurons may be particularly instructive (70). Several groups have demonstrated that a subpopulation of OPCs exists within the gray and white matter, which receive excitatory and inhibitory inputs from axons that elicit action potentials. The presence of excitatory neurotransmitter receptors on these cells makes them particularly susceptible to glutamate-mediated damage (41, 70). With the developmental maturation of OPCs to OLs, cells downregulate expression of the calcium-permeable ionotropic receptors, reducing their susceptibility to excitotoxic insult (71). Given our recent report demonstrating that FrCasE glial infection in the inferior colliculus causes rebound neuron hyperexcitability, coincident infection of NG2 glia would be expected to suspend those cells in the OPC state, rendering them persistently susceptible to excitoxic challenge. This hypothesis could explain the appearance of OPC cytoplasmic effacement with neurovirulent MLV infection noted here and previously (10, 14, 19). Thus, retrovirus-induced neurodegeneration may minimally require the alteration of at least two glial populations, one that results in neuronal hyperexcitability and one that interferes with OL differentiation and myelin repair. Although the ecotropic MLVs examined here are noninflammatory in the IRW mouse strain, it might be expected, in another strain where innate immune sensing of virus expression is robust or in animals with more fully developed acquired immune systems, that neuroinflammatory changes might constitute a third level of insult contributing to abnormal neuropathogenesis, highlighting the utility of the simple MLV models to differen-

NPCs. Note that many of these cells show endfeet contacts with blood vessels (arrowheads). Interestingly, mTom$^+$ cells with morphologies consistent with myelinating OLs were readily observed in animals transplanted with mock-infected NPCs at 14 dpt (lower left , arrows) but were not observed in animals transplanted with MLV-infected NPCs (cf. middle and right bottom panels). (B) Quantitative assessment of the total mTomato$^+$ cells at 7 and 14 dpt. The error bars in the graphs represent standard deviations. No significant engraftment differences were noted between transplant groups at 7 dpt (mock, $n = 5$ brains; FrCasE, $n = 3$ brains; Fr57E, $n = 5$ brains; one-way ANOVA with Tukey's multiple-comparison test). At 14 dpt, a highly significant difference (**, $P \leq 0.01$) was noted between mice transplanted with FrCasE- and mock-infected NPCs and a very highly significant difference (***, $P \leq 0.001$) was noted for FrCasE- versus Fr57E-infected NPCs (mock, $n = 6$ brains; FrCasE, $n = 3$ brains; Fr57E, $n = 6$ brains; one-way ANOVA with Tukey's multiple-comparison test). A significant difference ($P \leq 0.05$) was found between FrCasE at 7 dpt and FrCasE at 14 dpt (not shown), consistent with the proliferation of FrCasE NPCs upon engraftment. Note the different scales on the *y* axes for the two graphs. The lower graph shows quantitative analysis of mTom$^+$ cell morphologies at 7 and 14 dpt segregated into differentiated (multiple branched process bearing) and undifferentiated (amorphous, amoeboid, with few processes; e.g., asterisk in panel A). This analysis was done on the same cells counted in the upper graphs and was expressed as the fraction of differentiated cells found out of the total mTom$^+$ cells found in each brain. One-way ANOVA with Tukey's multiple-comparison test showed a significant difference between FrCasE and Fr57E NPCs at 7 dpt (*, $P < 0.05$) and very highly significant differences (***, $P < 0.001$) between FrCasE- and Fr57E-infected and mock- and Fr57E-infected NPCs at 14 dpt. No differences were noted between FrCasE- and mock-infected NPCs at either time point. (C) Representative example of a brainstem section from a mouse transplanted with FrCasE NPCs at 14 dpt immunostained with antibody directed to GFAP (green). Note localization of GFAP (green; middle) within the processes (arrows) of the engrafted mTom$^+$ cells (red; left) that appear yellow in the merged image (right). (D) Immunostaining for viral Env (green; top middle) and GFAP (white; bottom row) in a FrCasE NPC brainstem section at 14 dpt. Note that certain mTom$^+$ cells (red) show abundant Env expression (brackets), appearing yellow in the merged image (right), whereas other cells (arrows) have very little Env expression and appear largely red. Some of the Env$^+$ mTom$^+$ cells also express GFAP, consistent with astrocyte expression of virus *in vivo*. Note also the mTom-negative cells that also express Env (arrowheads), indicative of virus spread to host glia and endothelia. All images are single confocal planes. Scale bars, 20 μm.

tiate these processes from one another to assess mechanisms of neurodegeneration.

ACKNOWLEDGMENT

We thank Rochelle Cutrone for technical support of the project.

FUNDING INFORMATION

Northeast Ohio Medical University provided funding to William P. Lynch. HHS | National Institutes of Health (NIH) provided funding to William P. Lynch under grant number NS37614.

REFERENCES

1. **Gardner MB, Henderson BE, Officer JE, Rongey RW, Parker JC, Oliver C, Estes JD, Huebner RJ.** 1973. A spontaneous lower motor neuron disease apparently caused by indigenous type-C RNA virus in wild mice. J Natl Cancer Inst **51:**1243–1254.
2. **McCarter JA, Ball JK, Frei JV.** 1977. Lower limb paralysis induced in mice by a temperature-sensitive mutant of Moloney leukemia virus. J Natl Cancer Inst **59:**179–183.
3. **Munk C, Lohler J, Prassolov V, Just U, Stockschlader M, Stocking C.** 1997. Amphotropic murine leukemia viruses induce spongiform encephalomyelopathy. Proc Natl Acad Sci U S A **94:**5837–5842. http://dx.doi.org/10.1073/pnas.94.11.5837.
4. **Andrews JM, Andrews RL.** 1976. The comparative neuropathology of motor neuron diseaes, p 181–216. *In* Andrews JM, Johnson RT, Brazier MAB (ed), Amyotropic lateral sclerosis. Academic Press, New York, NY.
5. **Portis JL, Czub S, Garon CF, McAtee FJ.** 1990. Neurodegenerative disease induced by the Wild Mouse ecotropic retrovirus is markedly accelerated by long terminal repeat and *gag-pol* sequences from nondefective Friend murine leukemia virus. J Virol **64:**1648–1656.
6. **Gajdusek D.** 1992. Infectious amyloidoses: transthyretin familial amyloidotic polyneuropathy as a paradigm for genetic control of spontaneous generation of transmissible amyloids in CJD and other spongiform encephalopathies, p 503–523. *In* Roos RP (ed), Molecular neurovirology: pathogenesis of viral CNS infections. Humana Press, New York, NY.
7. **Jeffrey M, Gonzalez L.** 2004. Pathology and pathogenesis of bovine spongiform encephalopathy and scrapie. Curr Top Microbiol Immunol **284:**65–97.
8. **DesGroseillers L, Barrette M, Jolicoeur P.** 1984. Physical mapping of the paralysis-inducing determinant of a wild mouse ecotropic neurotropic retrovirus. J Virol **52:**356–363.
9. **Kay DG, Gravel C, Pothier F, Laperriere A, Robitalle Y, Jolicoeur P.** 1993. Neurological disease induced in transgenic mice expressing the env gene of the Cas-Br-E murine retrovirus. Proc Natl Acad Sci U S A **90:**4538–4542. http://dx.doi.org/10.1073/pnas.90.10.4538.
10. **Li Y, Cardona SM, Traister RS, Lynch WP.** 2011. Retrovirus-induced spongiform neurodegeneration is mediated by unique central nervous system viral targeting and expression of env alone. J Virol **85:**2060–2078. http://dx.doi.org/10.1128/JVI.02210-10.
11. **Yu YE, Choe W, Zhang W, Stoica G, Wong PK.** 1997. Development of pathological lesions in the central nervous system of transgenic mice expressing the env gene of ts1 Moloney murine leukemia virus in the absence of viral gag and pol genes and viral replication. J Neuorvirol **3:**274–282. http://dx.doi.org/10.3109/13550289709029468.
12. **Czub M, Czub S, McAtee FJ, Portis JL.** 1991. Age-dependent resistance to murine retrovirus-induced spongiform neurodegeneration results from central nervous system-specific restriction of virus replication. J Virol **65:**2539–2544.
13. **Czub M, McAtee FJ, Portis JL.** 1992. Murine retrovirus-induced spongiform encephalomyelopathy: host and viral factors which determine the length of the incubation period. J Virol **66:**3298–3305.
14. **Lynch WP, Czub S, McAtee FJ, Hayes SF, Portis JL.** 1991. Murine retrovirus-induced spongiform encephalopathy: productive infection of microglia and cerebellar neurons in accelerated CNS disease. Neuron **7:**365–379. http://dx.doi.org/10.1016/0896-6273(91)90289-C.
15. **Oldstone MB, Lampert PW, Lee S, Dixon FJ.** 1977. Pathogenesis of the slow disease of the central nervous system associated with WM 1504 E virus. I. Relationship of strain susceptibility and replication to disease. Am J Pathol **88:**193–212.
16. **Andrews JM, Gardner MB.** 1974. Lower motor neuron degeneration associated with type C RNA virus infection in mice: neuropathological features. J Neuropathol Exp Neurol **33:**285–307. http://dx.doi.org/10.1097/00005072-197404000-00007.
17. **Nagra RM, Masliah E, Wiley CA.** 1993. Synaptic and dendritic pathology in murine retroviral encephalitis. Exp Neurol **124:**283–288. http://dx.doi.org/10.1006/exnr.1993.1198.
18. **Morey MK, Wiley CA.** 1990. Immunohistochemical localization of neurotropic ecotropic murine leukemia virus in moribund mice. Virology **178:**104–112. http://dx.doi.org/10.1016/0042-6822(90)90383-3.
19. **Clase AC, Dimcheff DE, Favara C, Dorward D, McAtee FJ, Parrie LE, Ron D, Portis JL.** 2006. Oligodendrocytes are a major target of the toxicity of spongiogenic murine retroviruses. Am J Pathol **169:**1026–1038. http://dx.doi.org/10.2353/ajpath.2006.051357.
20. **Askovic S, McAtee FJ, Favara C, Portis JL.** 2000. Brain infection by neuroinvasive but avirulent murine oncornaviruses. J Virol **74:**465–473. http://dx.doi.org/10.1128/JVI.74.1.465-473.2000.
21. **Baszler TV, Zachary JF.** 1991. Murine retroviral neurovirulence correlates with an enhanced ability of virus to infect selectively, replicate in, and activate resident microglial cells. Am J Pathol **138:**655–671. (Erratum, **138:**1058.)
22. **Gravel C, Kay DG, Jolicoeur P.** 1993. Identification of the infected target cell type in spongiform myeloencephalopathy induced by the neurotropic Cas-Br-E murine leukemia virus. J Virol **67:**6648–6658.
23. **Nagra RM, Burrola PG, Wiley CA.** 1992. Development of spongiform encephalopathy in retroviral infected mice. Lab Invest **66:**292–302.
24. **Swarz JR, Brooks BR, Johnson RT.** 1981. Spongiform polioencephalomyelopathy caused by a murine retrovirus. II. Ultrastructural localization of virus replication and spongiform changes in the central nervous system. Neuropathol Appl Neurobiol **7:**365–380.
25. **Kay DG, Gravel C, Robitaille Y, Jolicoeur P.** 1991. Retrovirus-induced spongiform myeloencephalopathy in mice: regional distribution of infected target cells and neuronal loss occurring in the absence of viral expression in neurons. Proc Natl Acad Sci U S A **88:**1281–1285. http://dx.doi.org/10.1073/pnas.88.4.1281.
26. **Ligon KL, Kesari S, Kitada M, Sun T, Arnett HA, Alberta JA, Anderson DJ, Stiles CD, Rowitch DH.** 2006. Development of NG2 neural progenitor cells requires Olig gene function. Proc Natl Acad Sci U S A **103:**7853–7858. http://dx.doi.org/10.1073/pnas.0511001103.
27. **Nishiyama A, Lin XH, Giese N, Heldin CH, Stallcup WB.** 1996. Co-localization of NG2 proteoglycan and PDGF alpha-receptor on O2A progenitor cells in the developing rat brain. J Neurosci Res **43:**299–314. http://dx.doi.org/10.1002/(SICI)1097-4547(19960201)43:3<299::AID-JNR5>3.0.CO;2-E.
28. **Stallcup WB.** 1981. The NG2 antigen, a putative lineage marker: immunofluorescent localization in primary cultures of rat brain. Dev Biol **83:**154–165. http://dx.doi.org/10.1016/S0012-1606(81)80018-8.
29. **Nishiyama A, Suzuki R, Zhu X.** 2014. NG2 cells (polydendrocytes) in brain physiology and repair. Front Neurosci **8:**133. http://dx.doi.org/10.3389/fnins.2014.00133.
30. **Dawson MR, Polito A, Levine JM, Reynolds R.** 2003. NG2-expressing glial progenitor cells: an abundant and widespread population of cycling cells in the adult rat CNS. Mol Cell Neurosci **24:**476–488. http://dx.doi.org/10.1016/S1044-7431(03)00210-0.
31. **Pringle NP, Mudhar HS, Collarini EJ, Richardson WD.** 1992. PDGF receptors in the rat CNS: during late neurogenesis, PDGF alpha-receptor expression appears to be restricted to glial cells of the oligodendrocyte lineage. Development **115:**535–551.
32. **Dimou L, Simon C, Kirchhoff F, Takebayashi H, Gotz M.** 2008. Progeny of Olig2-expressing progenitors in the gray and white matter of the adult mouse cerebral cortex. J Neurosci **28:**10434–10442. http://dx.doi.org/10.1523/JNEUROSCI.2831-08.2008.
33. **Polito A, Reynolds R.** 2005. NG2-expressing cells as oligodendrocyte progenitors in the normal and demyelinated adult central nervous system. J Anat **207:**707–716. http://dx.doi.org/10.1111/j.1469-7580.2005.00454.x.
34. **Zhu X, Bergles DE, Nishiyama A.** 2008. NG2 cells generate both oligodendrocytes and gray matter astrocytes. Development **135:**145–157.
35. **Zhu X, Hill RA, Nishiyama A.** 2008. NG2 cells generate oligodendrocytes and gray matter astrocytes in the spinal cord. Neuron Glia Biol **4:**19–26.
36. **Komitova M, Zhu X, Serwanski DR, Nishiyama A.** 2009. NG2 cells are distinct from neurogenic cells in the postnatal mouse subventricular zone. J Comp Neurol **512:**702–716. http://dx.doi.org/10.1002/cne.21917.
37. **Nishiyama A, Komitova M, Suzuki R, Zhu X.** 2009. Polydendrocytes (NG2 cells): multifunctional cells with lineage plasticity. Nat Rev Neurosci **10:**9–22. http://dx.doi.org/10.1038/nrn2495.

38. **Lin SC, Huck JH, Roberts JD, Macklin WB, Somogyi P, Bergles DE.** 2005. Climbing fiber innervation of NG2-expressing glia in the mammalian cerebellum. Neuron **46:**773–785. http://dx.doi.org/10.1016/j.neuron.2005.04.025.
39. **Lin SC, Bergles DE.** 2004. Synaptic signaling between GABAergic interneurons and oligodendrocyte precursor cells in the hippocampus. Nat Neurosci **7:**24–32. http://dx.doi.org/10.1038/nn1162.
40. **Butt AM, Duncan A, Hornby MF, Kirvell SL, Hunter A, Levine JM, Berry M.** 1999. Cells expressing the NG2 antigen contact nodes of Ranvier in adult CNS white matter. Glia **26:**84–91.
41. **Karadottir R, Hamilton NB, Bakiri Y, Attwell D.** 2008. Spiking and nonspiking classes of oligodendrocyte precursor glia in CNS white matter. Nat Neurosci **11:**450–456. http://dx.doi.org/10.1038/nn2060.
42. **Butt AM, Hamilton N, Hubbard P, Pugh M, Ibrahim M.** 2005. Synantocytes: the fifth element. J Anat **207:**695–706. http://dx.doi.org/10.1111/j.1469-7580.2005.00458.x.
43. **Nishiyama A, Chang A, Trapp BD.** 1999. NG2+ glial cells: a novel glial cell population in the adult brain. J Neuropathol Exp Neurol **58:**1113–1124. http://dx.doi.org/10.1097/00005072-199911000-00001.
44. **Li Y, Davey RA, Sivaramakrishnan S, Lynch WP.** 2014. Postinhibitory rebound neurons and networks are disrupted in retrovirus-induced spongiform neurodegeneration. J Neurophysiol **112:**683–704. http://dx.doi.org/10.1152/jn.00227.2014.
45. **Muzumdar MD, Tasic B, Miyamichi K, Li L, Luo L.** 2007. A global double-fluorescent Cre reporter mouse. Genesis **45:**593–605. http://dx.doi.org/10.1002/dvg.20335.
46. **Nazarov V, Hilbert D, Wolff L.** 1994. Susceptibility and resistance to Moloney murine leukemia virus-induced promonocytic leukemia. Virology **205:**479–485. http://dx.doi.org/10.1006/viro.1994.1668.
47. **Mallon BS, Shick HE, Kidd GJ, Macklin WB.** 2002. Proteolipid promoter activity distinguishes two populations of NG2-positive cells throughout neonatal cortical development. J Neurosci **22:**876–885.
48. **Fuss B, Mallon B, Phan T, Ohlemeyer C, Kirchhoff F, Nishiyama A, Macklin WB.** 2000. Purification and analysis of in vivo-differentiated oligodendrocytes expressing the green fluorescent protein. Dev Biol **218:**259–274. http://dx.doi.org/10.1006/dbio.1999.9574.
49. **Dimcheff DE, Volkert LG, Li Y, DeLucia AL, Lynch WP.** 2006. Gene expression profiling of microglia infected by a highly neurovirulent murine leukemia virus: implications for neuropathogenesis. Retrovirology **3:**26. http://dx.doi.org/10.1186/1742-4690-3-26.
50. **Czub S, Lynch WP, Czub M, Portis JL.** 1994. Kinetic analysis of spongiform neurodegenerative disease induced by a highly virulent murine retrovirus. Lab Invest **70:**711–723.
51. **O'Doherty U, Swiggard WJ, Malim MH.** 2000. Human immunodeficiency virus type 1 spinoculation enhances infection through virus binding. J Virol **74:**10074–10080. http://dx.doi.org/10.1128/JVI.74.21.10074-10080.2000.
52. **Lynch WP, Sharpe AH, Snyder EY.** 1999. Neural stem cells as engraftable packaging lines can mediate gene delivery to microglia: evidence from studying retroviral env-related neurodegeneration. J Virol **73:**6841–6851.
53. **Lynch WP, Snyder EY, Qualtiere L, Portis JL, Sharpe AH.** 1996. Late virus replication events in microglia are required for neurovirulent retrovirus-induced spongiform neurodegeneration: evidence from neural progenitor-derived chimeric mouse brains. J Virol **70:**8896–8907.
54. **McAtee FJ, Portis JL.** 1985. Monoclonal antibodies specific for wild mouse neurotropic retrovirus: detection of comparable levels of virus replication in mouse strains susceptible and resistant to paralytic disease. J Virol **56:**1010–1022.
55. **Miller MJ, Kangas CD, Macklin WB.** 2009. Neuronal expression of the proteolipid protein gene in the medulla of the mouse. J Neurosci Res **87:**2842–2853. http://dx.doi.org/10.1002/jnr.22121.
56. **Lynch WP, Portis JL.** 2000. Neural stem cells as tools for understanding retroviral neuropathogenesis. Virology **271:**227–233. http://dx.doi.org/10.1006/viro.2000.0338.
57. **Pedraza CE, Monk R, Lei J, Hao Q, Macklin WB.** 2008. Production, characterization, and efficient transfection of highly pure oligodendrocyte precursor cultures from mouse embryonic neural progenitors. Glia **56:**1339–1352. http://dx.doi.org/10.1002/glia.20702.
58. **Laywell ED, Rakic P, Kukekov VG, Holland EC, Steindler DA.** 2000. Identification of a multipotent astrocytic stem cell in the immature and adult mouse brain. Proc Natl Acad Sci U S A **97:**13883–13888. http://dx.doi.org/10.1073/pnas.250471697.
59. **Lynch WP, Portis JL.** 1993. Murine retrovirus-induced spongiform encephalopathy: disease expression is dependent on postnatal development of the central nervous system. J Virol **67:**2601–2610.
60. **Liu N, Scofield VL, Qiang W, Yan M, Kuang X, Wong PK.** 2006. Interaction between endoplasmic reticulum stress and caspase 8 activation in retrovirus MoMuLV-ts1-infected astrocytes. Virology **348:**396–405.
61. **Qiang W, Kuang X, Liu J, Liu N, Scofield VL, Reid AJ, Jiang Y, Stoica G, Lynn WS, Wong PK.** 2006. Astrocytes survive chronic infection and cytopathic effects of the ts1 mutant of the retrovirus Moloney murine leukemia virus by upregulation of antioxidant defenses. J Virol **80:**3273–3284. http://dx.doi.org/10.1128/JVI.80.7.3273-3284.2006.
62. **Shikova E, Lin YC, Saha K, Brooks BR, Wong PK.** 1993. Correlation of specific virus-astrocyte interactions and cytopathic effects induced by ts1, a neurovirulent mutant of Moloney murine leukemia virus. J Virol **67:**1137–1147.
63. **Kremer D, Schichel T, Forster M, Tzekova N, Bernard C, van der Valk P, van Horssen J, Hartung HP, Perron H, Kury P.** 2013. Human endogenous retrovirus type W envelope protein inhibits oligodendroglial precursor cell differentiation. Ann Neurol **74:**721–732. http://dx.doi.org/10.1002/ana.23970.
64. **Hauser KF, Knapp PE.** 2014. Interactions of HIV and drugs of abuse: the importance of glia, neural progenitors, and host genetic factors. Int Rev Neurobiol **118:**231–313. http://dx.doi.org/10.1016/B978-0-12-801284-0.00009-9.
65. **Hahn YK, Podhaizer EM, Hauser KF, Knapp PE.** 2012. HIV-1 alters neural and glial progenitor cell dynamics in the central nervous system: coordinated response to opiates during maturation. Glia **60:**1871–1887. http://dx.doi.org/10.1002/glia.22403.
66. **Peng H, Sun L, Jia B, Lan X, Zhu B, Wu Y, Zheng J.** 2011. HIV-1-infected and immune-activated macrophages induce astrocytic differentiation of human cortical neural progenitor cells via the STAT3 pathway. PLoS One **6:**e19439. http://dx.doi.org/10.1371/journal.pone.0019439.
67. **Douville R, Liu J, Rothstein J, Nath A.** 2011. Identification of active loci of a human endogenous retrovirus in neurons of patients with amyotrophic lateral sclerosis. Ann Neurol **69:**141–151. http://dx.doi.org/10.1002/ana.22149.
68. **Li W, Lee MH, Henderson L, Tyagi R, Bachani M, Steiner J, Campanac E, Hoffman DA, von Geldern G, Johnson K, Maric D, Morris HD, Lentz M, Pak K, Mammen A, Ostrow L, Rothstein J, Nath A.** 2015. Human endogenous retrovirus-K contributes to motor neuron disease. Sci Transl Med **7:**307ra153. http://dx.doi.org/10.1126/scitranslmed.aac8201.
69. **Kang SH, Li Y, Fukaya M, Lorenzini I, Cleveland DW, Ostrow LW, Rothstein JD, Bergles DE.** 2013. Degeneration and impaired regeneration of gray matter oligodendrocytes in amyotrophic lateral sclerosis. Nat Neurosci **16:**571–579. http://dx.doi.org/10.1038/nn.3357.
70. **Bergles DE, Jabs R, Steinhauser C.** 2010. Neuron-glia synapses in the brain. Brain Res Rev **63:**130–137. http://dx.doi.org/10.1016/j.brainresrev.2009.12.003.
71. **De Biase LM, Nishiyama A, Bergles DE.** 2010. Excitability and synaptic communication within the oligodendrocyte lineage. J Neurosci **30:**3600–3611. http://dx.doi.org/10.1523/JNEUROSCI.6000-09.2010.